NATIONAL TECHNICAL UNIVERSITY OF ATHENS
DEPARTMENT OF NAVAL ARCHITECTURE AND MARINE ENGINEERING

A method for predicting the flow around the stern of double ship hulls

by

George D. Tzabiras[1]
Theodore A.Loukakis[2]

January 1983

(1) Research Assistant N.T.U.A.

(2) Professor of Ship Theory, Department of Naval Architecture and Marine Engineering, National Technical University of Athens (N.T.U.A.)

ABSTRACT

The present work deals with the numerical calculation of the turbulent flow around double ship hulls, with emphasis to the stern region and the wake. A new coordinate system has been developed for the application of the SIMPLE Algorithm of Patankar and Spalding 1972, applied for external flows. Comparison of the numerical results with the experimental data is presented for two test cases.

NOMENCLATURE

α_n	coefficients of conformal transformation
k	turbulent kinetic energy
l_η, l_ξ	metrics of the curvilinear system
l_m	mixing length
p, p_o	static pressures
r, θ, z	polar coordinates
u_j	mean velocity components in Cartesian coordinates
u, v, w	mean velocity components in cylindrical and curvilinear coordinate system
x_j	Cartesian coordinates
$A_{N,S,E,W,P,U}$	coefficients of difference equations
C_p	pressure coefficient
C_F	friction coefficient
C_1, C_2, C_D $P_{r,k}, P_{r,\varepsilon}$	constants for k-ε equations
L	length of the model
Re	Reynolds Number
S_ϕ	source terms
U_∞	velocity at infinite
X	distance from the midship section

Greek Symbols

δ	boundary layer thickness
ε	dissipation rate of k
μ	fluid viscosity
μ_e	effective viscosity
ξ, η, ζ	cylindrical and curvilinear coordinates
ρ	fluid density
$\overline{\rho u_i' u_j'}$	Reynolds stresses
σ_{ij}	stress tensor in Cartesian coordinates
τ_{ij}	stress tensor in curvilinear coordinates
τ_w	wall shear stress
ϕ	variable

1. INTRODUCTION

As the estimation of the flow parameters around the stern of ships becomes very useful for design, many numerical methods have been developed for the calculation of the three-dimensional turbulent boundary layer around double models (see e.g. SSPA - ITTC Workshop 1980). However, due to inadequecies of either the physical modelling of turbulence or the numerical methods used, there exist still difficulties for the accurate solution of the problem.

Regardless of the turbulence modelling, another major problem in the calculation of a thick three dimensional boundary layer at the stern of a double model is the strong viscous-inviscid flow interaction. This interaction alters both the external velocity boundary condition and the pressure field within the thick boundary layer region, in relation to those predicted by a potential flow solution for the actual body. Thus, the usual numerical methods, which do not take into account this strong influence (specially of the pressure field), fail to predict (or are unable to calculate) the flow parameters at the stern region.

On the other hand when the external boundary of the solution domain is placed far enough from the actual body, the change of the boundary conditions there (from their initial potential flow estimation) is expected to be of minor importance for the numerical solution. This means that the main difficulty of the viscous - inviscid interaction problem is the estimation of the pressure field. In 1978

Abdelmeguid, Markatos and Spalding obtained for the first time such a solution by applying the Partially Parabolic method, which is described in the next Section. However, the results given by Muraoka, who applied the above method for the SSPA-ITTC Workshop 1980, were not satisfactory when compared to other methods of calculation or the experimental results. A reason for this discrepancy is the influence of the finite difference grid that was used (distored cylindrical system) on the numerical solution of the problem. Since the method is more expensive than the usual ones, its usefulness becomes questionalbe and the need of a more suitable coordinate system is apparent.

In this work we present a new coordinate system for the application of the Partially Parabolic method and the results obtained for two test cases. The model of turbulence used is the well known k-ε model (see for example Launder and Spalding 1974).

2. THE FUNDAMENTALS OF THE PARTIALLY PARABOLIC METHOD

In this Section we present for completness the fundamentals of the Partially Parabolic Method (e.g. Abdelmeguid-Markatos-Spalding 1978, Muraoka 1980, Markatos-Malin-Tatchell 1980) for the calculation of the turbulent flow around double ship hulls.

The governing time-averaged equations, for three-dimensional turbulent flows in Cartesian coordinates are:

Continuity equation

$$\frac{\partial}{\partial x_j}(\rho u_j)=0 \quad j=1,2,3 \qquad (1)$$

Momentum equations

$$\frac{\partial}{\partial x_j}(\rho u_i u_j) = \frac{-\partial p}{\partial x_i} + \frac{\partial}{\partial x_j}(\sigma_{ij}) \quad i,j=1,2,3 \qquad (2)$$

where (u_1,u_2,u_3) are the mean values of the velocity components in Cartesian coordinates (x_1,x_2,x_3), p the mean value of the pressure and ρ the density of the fluid. In relations (2), σ_{ij} denotes the stress tensor including the terms of both viscous stresses and corresponding double velocity correlations, that is

$$\sigma_{ij} = \mu\left(\frac{\partial u_i}{\partial x_j}+\frac{\partial u_j}{\partial x_i}\right) - \rho\overline{u_i' u_j'} \qquad (3)$$

Under the concept of turbulent viscosity, the tensor σ_{ij} may be expressed as

$$\sigma_{ij}=\mu_e\left(\frac{\partial u_i}{\partial x_j}+\frac{\partial u_j}{\partial x_i}\right) \qquad (4)$$

where μ_e is the effective turbulent viscosity which (e.g. Launder and Spalding 1974) is given by

$$\mu_e = \mu+\mu_t = \mu + C_D.\rho.k^2/\varepsilon \qquad (5)$$

In this relation C_D is a constant, k is the turbulent kinetic energy and ε its dissipation rate. Since the estimation of μ_e requires known values of k and ε, two more equations are involved respectively. These are the well known equations of the k-ε Model of turbulence

$$\frac{\partial}{\partial x_j}(\rho u_j k) = \mu_t\left(\frac{\partial u_i}{\partial x_j}+\frac{\partial u_j}{\partial x_i}\right)\frac{\partial u_i}{\partial x_j}+\frac{\partial}{\partial x_j}\left(\frac{\mu t}{P_{r,k}}\frac{\partial k}{\partial x_j}\right)-\rho\varepsilon \tag{6}$$

$$\frac{\partial}{\partial x_j}(\rho u_j \varepsilon) = \frac{\partial}{\partial x_j}\left(\frac{\mu t}{P_{r,\varepsilon}}\frac{\partial \varepsilon}{\partial x_j}\right)+C_1\frac{\varepsilon}{k}\mu_t\left(\frac{\partial u_i}{\partial x_j}+\frac{\partial u_j}{\partial x_i}\right)\frac{\partial u_i}{\partial x_j} - C_2\rho\frac{\varepsilon^2}{k} \tag{7}$$

The experimental values for C_D, C_1, C_2, $P_{r,k}$, $P_{r,\varepsilon}$ are given in Table 1.

C_D	C_1	C_2	$P_{r,k}$	$P_{r,\varepsilon}$
0.09	1.44	1.92	1.	1.23

Table 1 Constants for k-ε equations

If there exists a dominant velocity component of the flow (in the x_1 direction in our case) and the diffusion of any transferable quantity Φ is negligible along this direction, the following assumptions relative to equations (2), (6) and (7) may be adopted

1) $\frac{\partial^2\Phi}{\partial x_1^2} = 0, \quad \sigma_{11}=0$

2) Terms including $\frac{\partial u_2}{\partial x_1}$ and $\frac{\partial u_3}{\partial x_1}$ are neglected in the viscous stresses σ_{12} and σ_{13} for the x_1 momentum equation

3) Terms including σ_{12}, σ_{13}, are neglected for the x_2 and x_3 momentum equations.

These assumptions correspond to the statement of the higher order boundary layer equations, which may be derived from the initial set of equations (2), (6) and (7). The resulting equations are parabolic in the x_1 direction and therefore can be solved in a single sweep of the flow domain, if the pressure p is known or may be derived from the usual potential flow solutions.

However, as mentioned in Section 1, the usual potential methods fail to predict accurately the pressure field in regions of thick boundary layers, such as near the stern of ships. In order to overcome the problem of pressure estimation Abdelmeguid et al 1978, used the Partially Parabolic method of Patankar and Spalding 1972, which is often refered to as the SIMPLE Algorithm. In this method the pressure field is treated as fully elliptic, which means that several sweeps of the flow domain are necessary until numerical convergence is achieved. (The values of the pressure in a control volume are altered in each sweep so that the continuity equation (1) is satisfied). Abdelmeguid et al 1978, used a distorted cylindrical system, whose axis z coincides with the axis of symmetry of the double model. The momentum and k-ε equations

are written in cylindrical coordinates and then transformed in a non-orthogonal system (ξ,η,ζ), which is derived using relations (see Figs.1,2).

$$\eta = \frac{r-r_S}{r_N-r_S}, \quad \xi = \frac{\theta}{\pi/2}, \quad \zeta=z$$

The flow field is covered by a finite-difference grid and the flow variables are stored in grid nodes as described by Patankar and Spalding 1972. The velocity components u,v,w correspond to the angular, radial and longitudinal direction of the initial cylindrical coordinate system. The method of numerical solution follows the basic concepts of the SIMPLE Algorithm, suitably applied for external flows.

However, the use of this distorted cylindrical system introduces certain difficulties with regard to the numerical solution. This is because the "radial"sides of the finite difference cells may deviate considerably from the normal near to the hull surface and the circumferential component of the velocity u may be at large angles to the normal at the hull surface. The application of the finite difference scheme to such a geometry may result in large errors of the numerical solution.

These problems usually appear in regions of stern sections, where rapid changes in the crossflow velocity occur (streamline convergence, vortex sheet separation). In these cases, wrong estimation of the flow parameters at these sections affects definitivelly the solution. Since the pressure field is treated as elliptic, such errors are introduced

in both the downstream and upstream direction relative to the above sections. In fact the results presented by Muraoka, at SSPA 1980, show that there exists a problem even in the qualitative prediction of the cross flow velocity at stern sections.

Trying to overcome this difficulty Markatos etal 1980, used a modified distorted cylindrical system by shifting the axis z of the original system (Fig.3) and so reducing the skewness of the cells close to the hull. However the modified grid arrangement is worse that the original one for the after most part of a cruiser-type stern and also for most of the rest of the sections of the hull.

This questionable application of the distored cylindrical grid led us to the development of a new coordinate system in our effort to predict more accurately the turbulent flow around the stern of double ship hulls.

3. THE NEW COORDINATE SYSTEM AND THE CORRESPONDING EQUATIONS.

The Coordinate System

In the present method we use a local orthogonal curvilinear coordinate system (ξ,η,ζ) for every section in the solution domain (Fig. 4). The direction ζ is always parallel to the axis of symmetry of the double model, that is the lines (ξ,η) form a two dimensional orthogonal curvilinear system ,where the first line η=const coinsides with the section contour. The orthogonal set of lines ξ and η for each station is generated by the method of conformal mapping as briefly described in the sequel. The velocity components (u,v) refer to the local directions (ξ,η) of the coordinate system, so that near the hull surface the u and v components are almost parallel and normal to it. In this way we succeed in eliminating the errors due to the skewness of the near hull cells as described in Section 2. Another advantage of the proposed system is that the grid nodes lying on the hull may follow arbitrary contours in the longitudinal direction. This allows for a better grid arrangement in regions of interest.

The orthogonal grid (ξ,η) on each station is generated by conformal mapping of the station contour on a unit circle. (Von Kerczeck,1969). If z is the plane of the station and ζ the plane of the corresponding circle, the mapping function is

$$z = \sum_{n=1}^{N} \alpha_n \zeta^{(3-2n)} \qquad (8)$$

The coefficients α_n are calculated as proposed by Von Kerczeck 1969. Usually for the fore and midship stations six coefficients are enough for an adequate contour representation, while nine coefficients are needed for the stern stations. If the mapping function for each station is known, the corresponding (ξ,η) grid on z plane is generated by conformal mapping of the orthogonal (r,θ) gid on the circle plane ζ (Fig. 4).

A problem is raised at the stern stations, where a rapid change in the ship draft exists. As it is shown in Fig. 5, if the above method is applied to the adjacent sections z'and z, which have different drafts, then the point A_1 of section z'corresponds to the point B of section z for the finite difference grid in the longitudinal direction. This means that the geometry of a control volume near and between the points A_1 and B will change rabidly in the longitudinal direction. This is quite inappropriate for the numerical solution scheme. To overcome this difficulty we used the following procedure:

Since we want the point A on the z plane to have the same draft as A_1 on z'plane for our difference grid, we find first the point A'on the unit circle plane ζ which corresponds to A according to the inverse of the mapping (8). Then we apply the conformal mapping $w=\zeta+1/\zeta$ which transforms the unit circle on ζ to a line segment 0"B" on the w plane. The point A'is mapped on A". If we perform an inverse transformation of the line segment 0"A"on

a unit circle, then an orthogonal grid (ξ_w,η_w) on the w plane as shown in Fig. 5 , can be easily generated by the (r,θ) grid of that circle. Using now the inverse mapping w^{-1} and the initial mapping (8),we obtain the desired (ξ,η) grid on the z plane from the (ξ_w,η_w) grid on the w plane.

In Fig. 6 are shown three(ξ,η) orthogonal curvilinear gridsfor stern sections of the SSPA Model of Larsson 1975 and one for an adjacent wake section.

The Governing Equations

In the local coordinate system of each station the momentum equations as well the equations for k and ε are written as follows (see for example Antonopoulos 1979)

$$\frac{1}{l_\xi l_\eta}\frac{\partial}{\partial\xi}(\rho u l_\eta \Phi)+\frac{1}{l_\xi l_\eta}\frac{\partial}{\partial\eta}(\rho v l_\xi \Phi)+\frac{\partial}{\partial\zeta}(\rho w\Phi)$$

$$-\frac{1}{l_\xi l_\eta}\frac{\partial}{\partial\xi}\left(\Gamma\phi_e\frac{l_\eta}{l_\xi}\frac{\partial\Phi}{\partial\xi}\right)-\frac{1}{l_\xi l_\eta}\frac{\partial}{\partial\eta}\left(\Gamma\phi_e\frac{l_\xi}{l_\eta}\frac{\partial\Phi}{\partial\eta}\right)-S_\phi=0 \qquad (9)$$

where Φ=u,v,w,k,ε and l_ξ, $l_\eta$are the metrics of the curvilinear system along the ξ and η directions. Expressions of S_ϕ and $\Gamma\phi_e$ for each variable Φ are given in Tables 2 and 3. The term G, appearing in the expression of S_ϕ for k and ε in Table 2, is expressed as

$$G=\frac{1}{2\mu_e}\left[\tau_{\xi\xi}^2+\tau_{\eta\eta}^2+2(\tau_{\xi\eta}^2+\tau_{\xi\zeta}^2+\tau_{\eta\zeta}^2)\right] \qquad (10)$$

where

$$\tau_{\xi\xi}=2\mu_e\left(\frac{1}{l_\xi}\frac{\partial u}{\partial\xi}+\frac{v}{l_\xi l_\eta}\frac{\partial l_\xi}{\partial\eta}\right) \qquad (11)$$

$$\tau_{\eta\eta}=2\mu_e\left(\frac{1}{l_\eta}\frac{\partial v}{\partial\eta}+\frac{u}{l_\xi l_\eta}\frac{\partial l_\eta}{\partial\xi}\right)$$

$$\tau_{\xi\eta} = \mu_e \left(\frac{1}{l_\xi} \frac{\partial v}{\partial \xi} + \frac{1}{l_\eta} \frac{\partial u}{\partial \eta} - \frac{v}{l_\xi l_\eta} \frac{\partial l_\eta}{\partial \xi} - \frac{u}{l_\xi l_\eta} \frac{\partial l_\xi}{\partial \eta} \right)$$

$$\tau_{\xi\zeta} = \mu_e \left(\frac{1}{l_\xi} \frac{\partial w}{\partial \xi} \right)$$

$$\tau_{\eta\zeta} = \mu_e \left(\frac{1}{l_\eta} \frac{\partial w}{\partial \eta} \right)$$

In the equations (9), (10) and (11) we have taken into account the assumptions of the Section 2 relative to the parabolic nature of the boundary layer equations.

The finite difference grid used for the numerical solution of equations (9) is formed in the same way as in the method of Abdelmeguid et al 1978, for the distored cylindrical system. But the control volume for each variable Φ is based on the local coordinate systems of adjacent stations (Fig. 7).

4. THE SOLUTION ALGORITHM AND THE BOUNDARY CONDITIONS

4.1. The Solution Algorithm

The method for numerical solution of equations (8) follows the procedure described by Patankar and Spalding, 1972. The general transport equation (8) is integrated in the arbitrary control volume for each variable, giving a finite difference equation of the Form:

$$A_P\Phi_P = A_N\Phi_N + A_S\Phi_S + A_E\Phi_E + A_W\Phi_W + A_U\Phi_U + S_\phi \qquad (12)$$

where $\Phi = u,v,w,p,k,\varepsilon$

The notation P,N,S,E,W,U stands for the grid nodes shown in Fig. 7 . Since the coefficients A_i are generally functions of the variable Φ, the system of equations (12) is nonlinear and an iterative solution must be applied. The solution algorithm follows the next steps:

1. The values of the coefficients of equations (11) at each section are evaluated on the basis of the known values of Φ at the upstream station. Then, the u,v,w momentum equations are solved.

2. The pressure field in the section under consideration is corrected so that the continuity equation is satisfied. The cross flow components u and v are corrected respectively.

3. The velocity components u,v,w derived in 1 and 2 are used for the solution of the k and ε equations, for the same section.

4. Since equations (12) are elliptic in the (ξ,η)plane,

steps 1 to 3 are repeated until numerical convergence is achieved. The coefficients A_i are updated in every iteration from the values of the previous one. This is a different procedure than the initial SIMPLE Algorithm, where the values of A_i are estimated from the known variables of Φ at the upstream section. The necessity of this iterative solution is evident since the geometry of the (ξ,η) grid varies considerably in the region of the stern.

5. Since the pressure field is unknown a priori in the present algorithm, steps 1 to 4 are repeated for all sections, until numerical convergence of the pressure field is achieved.

4.2 The Boundary Conditions

Inlet Plane

Since we are mainly concerned with the stern flow prediction, the inlet plane is placed near the midship section. Up to the middle of the hull and even further downstream the usual integral methods are adequate to give the initial values of the u,v,w components within the boundary layer. Moreover the pressure field in this region is adequately estimated from the potential flow solution . Usually only the boundary layer thickness δ is needed from an integral method and the velocities u, w are estimated by the 1/7 power law from their known values at the edge of boundary layer, while the v component is assumed zero. The values of u, v, w outside the boundary layer are calculated by the potential flow solution for the actual body.

The proposed by Muraoka 1979 values for k and ε are used at the inlet plane, that is k is given by Klebanoff's 1952 data

for flat plate and ε is given by relation

$$\varepsilon = C_D^{3/4} \, k^{3/2} / lm$$

where lm is calculated after Bradshaw et al, 1967.

Free Boundary

The velocity components and the pressure at the free boundary are calculated from the potential flow solution for the actual Body. For k and ε it is assumed that

$$\frac{\partial k}{\partial \eta} = \frac{\partial \varepsilon}{\partial \eta} = 0$$

The free boundary is selected so that its distance from the body surface is at least twise the boundary layer thickness at each station in order to avoid large influence of the displacement effect on the boundary conditions.

Hull Surface

On the hull surface the no slip condition u=v=w=0 is applied, while at the adjacent control volumes the wall function method of Patankar and Spalding 1972, is used for the u,w and k,ε equations. For k and ε a zero diffusive flux is assumed on the boundary.

Symmetry Planes

Since the solution domain is restricted to the 1/4 of the double model there exist two symmetry planes,that is the water plane and the center plane. The boundary conditions there,are as follows

$$u = 0$$

$$\frac{\partial \Phi}{\partial \xi} = 0 \qquad \Phi = v, w, p, k, \varepsilon$$

Exit Plane

The exit plane is usually located far downstream from the aft end of the ship and the necessary values for pressure are given by linear extrapolation of the results obtained in the previous iteration of the solution.

5. RESULTS AND DISCUSSION

The present method was tested for the two cases of double models used at the SSPA - ITTC Workshop on Ship Boundary Layers, Göteborg, 1980. These are the SSPA Liner Model (Reynolds No.= 5×10^6) tested by Larsson, 1975 and the HSVA Tanker Model, (Reynolds No.= 6.6×10^6) tested by Hoffmann, 1976. The body plans of the two models are shown in Fig. 8.

Since the convergence of the method is rapid in the flow region before the aft-end of the hull, the solution domain is separated in two overlaping regions. Results are taken from the first rapid-convergence region at a certain station as input for the second region. The number of ξ and η grid points as well as the position of the first and last sections of each region for the two cases are given in Table 4.

For the SSPA Model measurements of pressure coefficients $C_p = \frac{p-p_o}{\frac{1}{2}\rho U_\infty^2}$ and friction coefficients $C_f = \frac{\tau_w}{\frac{1}{2}\rho U_\infty^2}$ are available along the eight potential flowlines shown in Fig. 8 . In Figs 9a and 9b the measured and calculated values of C_p are presented for each line at the stern of the SSPA Model. The doted line corresponds to the calculation of C_p by the potential flow Program of Hess and Smith 1962, and the continous line to the calculation by the proposed method. Near the stern, the proposed method gives satisfactory predictions for C_p, while the potential flow calculations give large overestimations of it. In Figs. 10a and 10b the measured and calculated values of C_f are presented for the same flowlines.

Finally in Figs. 11 and 12 the measured and calculated values for the longitudinal and crosswise velocity profiles are presented for the flowlines 1, 2 and 5 at the stations 2X/L=0.5, 0.7 and 0.9. The vertical scale y/δ refers to the fraction of the wall distance to the measured boundary layer thickness δ. A good agreement is observed between the measured and calculated values.

For the HSVA Tanker Model the calculated and measured values of the longitudinal and crosswise velocity profiles are presented in Fig.13 for the points 182,183,185 at 2X/L=.884 shown in Fig. 8. The discrepancies here between the calculated and measured results are at point 183, where the phenomenon of "shear separation" occurs (Odabasi 1980). But this is considered to be rather a turbulence modelling problem and happens only at low Reynolds numbers, which means that at the Reynolds numbers of interest a better result is expected from our computation scheme.

Finally, in Figs.14a,b,c,d the directions of crossflow velocities are shown for four sections of the solution domain and there is a good qualitative agreement with the experiments by Kux and Wieghardt, 1980.

Although the results obtained seem to be promising there is still a thorough investigation to be made in order to test:

1. The number and the arrangement of the grid nodes on the accuracy of the numerical solution.

2. The influence of the imposed external boundary conditions on the solution.

3. The examination of the basic assumptions of the parabolic boundary layer equations by adding the terms which have been neglected. This means that the equations (9) will be elliptic, increasing greatly the computation cost.

4. The comparison of numerical results for Reynolds stresses with experimental data, so that the applicability of the k-ε model in calculating the turbulent flow around ships will be examined.

References

1. Abdelmeguid A.M., Markatos N.C.G., Spalding D.B. "A Method of Predicting Three-Dimensional Turbulent Flows around Ship's Hulls" International Symposium on Ship Viscous Resistance, SSPA, Göteborg, 1978

2. Antonopoulos K. "Prediction of Flow and Heat Transfer in Rod Bundles" PHD Thesis, Imperial College, 1979

3. Bradshaw P., Ferris D.H., Atwell N.P. "Calculation of Boundary Layer Development Using the Turbulent Energy Equation" JFM Vol.28, 1967

4. Hess J.L., Smith A.M.O. "Calculation of Non-Lifting Potential Flow about Arbitrary Three Dimensional Bodies" Douglas A.C., 1962

5. Hoffmann, H.P."Untersuchung der 3-dimensionalen, turbulenten Grezschicht an einem Schiffdoppelmodell im Windkanal"Institut für Schiffbau der Universität Hamburg, Bericht Nr 343, 1976

6. Von Kerczeck C., Tuck E.O. "The Representation of Ship Hulls by Conformal Mapping Functions" JSR, 1969

7. Klebanoff P.S. "Characteristics of Turbulence in a Boundary Layer with zero Pressure Gradient"NACA Rept. 1247, 1952

8. Kux J. and Wieghardt K. "Three dimensional Measurements near the Stern of a Double Model of a Ship"Institut für Schiffbau der Universistät Hamburg, 1980

9. Larrson L. "Boundary Layers of Ships" PHD Thesis,Göteborg, 1975

10. Launder B.E., Spalding D.B. "The Numerical Computation of Turbulent Flows" Computer Methods in Applied Mechanics and Engineering, 1974

11. Markatos N.C., Malin M.R., Tatchell D.G. "Computer Analysis of Three-Dimensional Turbulent Flows around Ship's Hulls" Proceedings of the Institution of Mechanical Engineers Vol. 194, 1980

12. Muraoka K. "Examination of a 2-Equation Model of Turbulence for Calculating the Viscous Flow around Ships" Transactions of the West-Japan Society of Naval Architects, No. 58, 1979

13. Muraoka K. "Calculation of Thick Boundary Layer and Wake of Ships by a Partially Parabolic Method" 13 ONR, Tokyo, 1980

14. Odabaşi A.Y., Şaylan O."GEMAK-A Method for Calculating the Flow around Aft-End of Ships"13 ONR, Tokyo, 1980

15. Patankar S.V., Spalding D.B. "A Calculation Procedure for Heat, Mass and Momentum Transfer in Three-Dimensional Parabolic Flows" Int.J.Heat Mass Transfer, Vol.15, 1972

16. Proceedings of "SSPA-ITTC Workshop on Ship Boundary Layers" Göteborg, 1980

Φ	S_ϕ
u	$$-\frac{1}{l_\xi}\frac{\partial p}{\partial \xi}-\frac{\rho uv}{l_\xi l_\eta}\frac{\partial l_\xi}{\partial \eta}+\frac{\rho v^2}{l_\xi l_\eta}\frac{\partial l_\eta}{\partial \xi}$$ $$+\frac{1}{l_\xi l_\eta}\frac{\partial}{\partial \xi}\left[\frac{l_\eta}{l_\xi}\mu_e\left(\frac{\partial \mu}{\partial \xi}+\frac{2v}{l_\eta}\frac{\partial l_\xi}{\partial \eta}\right)\right]$$ $$+\frac{1}{l_\xi l_\eta}\frac{\partial}{\partial \eta}\left[l_\xi\mu_e\left(\frac{1}{l_\xi}\frac{\partial v}{\partial \xi}-\frac{v}{l_\xi l_\eta}\frac{\partial l_\eta}{\partial \xi}-\frac{u}{l_\xi l_\eta}\frac{\partial l_\xi}{\partial \eta}\right)\right]$$ $$+\frac{\mu_e}{l_\xi l_\eta}\left(\frac{1}{l_\xi}\frac{\partial v}{\partial \xi}+\frac{1}{l_\eta}\frac{\partial u}{\partial \eta}-\frac{v}{l_\xi l_\eta}\frac{\partial l_\eta}{\partial \xi}-\frac{u}{l_\xi l_\eta}\frac{\partial l_\xi}{\partial \eta}\right)\frac{\partial l_\xi}{\partial \eta}$$ $$-\frac{2\mu_e}{l_\xi l_\eta}\left(\frac{1}{l_\eta}\frac{\partial v}{\partial \eta}+\frac{u}{l_\xi l_\eta}\frac{\partial l_\eta}{\partial \xi}\right)\frac{\partial l_\eta}{\partial \xi}$$
v	$$-\frac{1}{l_\eta}\frac{\partial p}{\partial \eta}-\frac{\rho uv}{l_\xi l_\eta}\frac{\partial l_\eta}{\partial \xi}+\frac{\rho u^2}{l_\xi l_\eta}\frac{\partial l_\xi}{\partial \eta}$$ $$+\frac{1}{l_\xi l_\eta}\frac{\partial}{\partial \eta}\left[\frac{l_\xi}{l_\eta}\mu_e\left(\frac{\partial v}{\partial \eta}+\frac{2u}{l_\xi}\frac{\partial l_\eta}{\partial \xi}\right)\right]$$ $$+\frac{1}{l_\xi l_\eta}\frac{\partial}{\partial \eta}\left[l_\eta\mu_e\left(\frac{1}{l_\eta}\frac{\partial u}{\partial \eta}-\frac{v}{l_\xi l_\eta}\frac{\partial l_\eta}{\partial \xi}-\frac{u}{l_\xi l_\eta}\frac{\partial l_\xi}{\partial \eta}\right)\right]$$ $$+\frac{\mu_e}{l_\xi l_\eta}\left(\frac{1}{l_\xi}\frac{\partial v}{\partial \xi}+\frac{1}{l_\eta}\frac{\partial u}{\partial \eta}-\frac{v}{l_\xi l_\eta}\frac{\partial l_\eta}{\partial \xi}-\frac{u}{l_\xi l_\eta}\frac{\partial l_\xi}{\partial \eta}\right)\frac{\partial l_\eta}{\partial \xi}$$ $$-\frac{2\mu_e}{l_\xi l_\eta}\left(\frac{1}{l_\xi}\frac{\partial u}{\partial \xi}+\frac{v}{l_\xi l_\eta}\frac{\partial l_\xi}{\partial \eta}\right)\frac{\partial l_\xi}{\partial \eta}$$
w	$$-\frac{\partial p}{\partial \zeta}$$
	$G-\rho\varepsilon$
	$$C_1 G\frac{\varepsilon}{k}-C_2\rho\frac{\varepsilon^2}{k}$$

Table 2 Source terms for momentum and k-ε equations

Φ	u,v,w	k	ε
$\Gamma_{\phi e}$	$\mu_e=\mu+\mu t$	$\frac{\mu_e}{P_{r,k}}$	$\frac{\mu_e}{P_{r,\varepsilon}}$

Table 3 Γ_ϕ for momentum and k-ε equations

	SSPA Model		HSVA Model	
	First Region	Second Region	First Region	Second Region
ξ grid points	19	19	19	19
η grid points	19	19	19	19
ζ grid points	26	23	21	24
first section	2X/L=0.15	2X/L =0.75	2X/L= 0.4	2X/L=0.8
last section	2X/L=0.9	2X/L =1.4	2X/L=0.9	2X/L=1.4
No of Sweeps for convergence	8	30	10	30

Table 4 Grid particulars for the two test cases

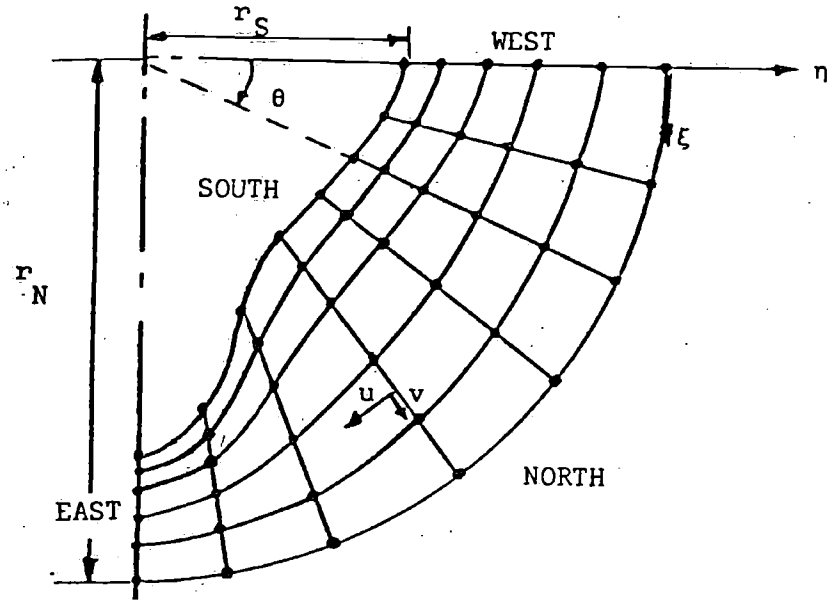

Fig. 1 The distorted cylindrical system: cross section

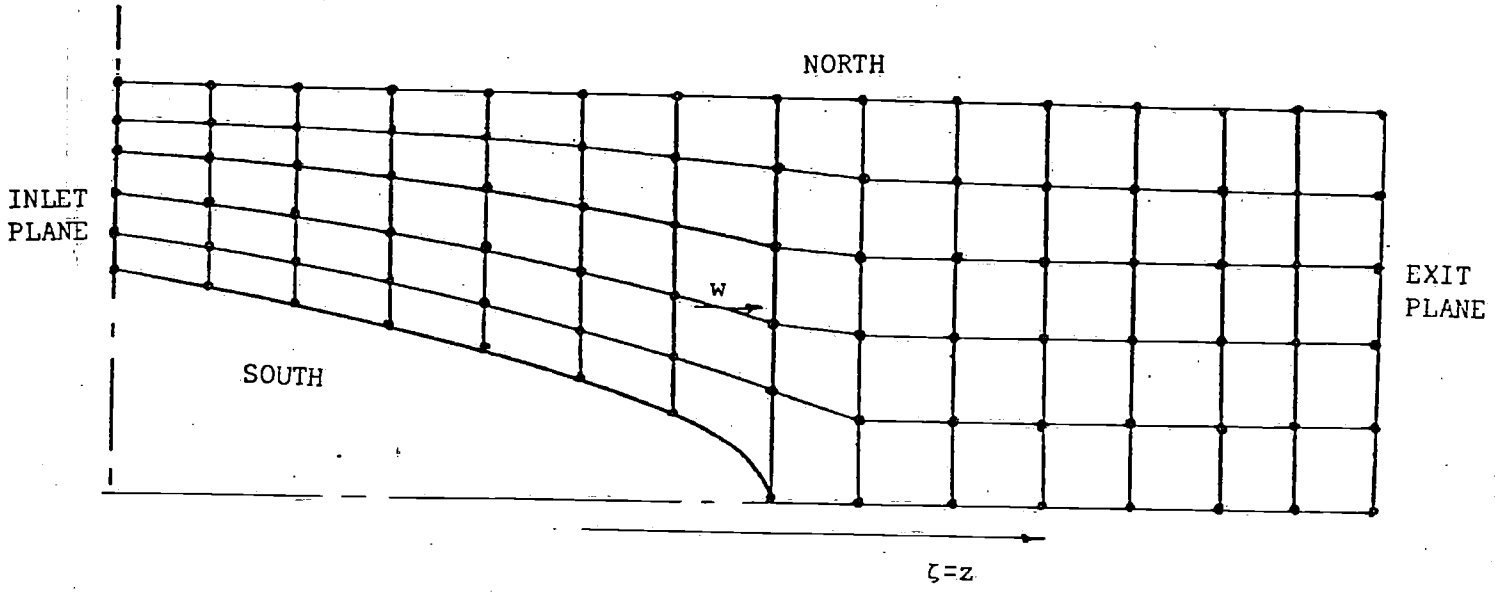

Fig. 2. The distorted cylindrical system: longitudinal section

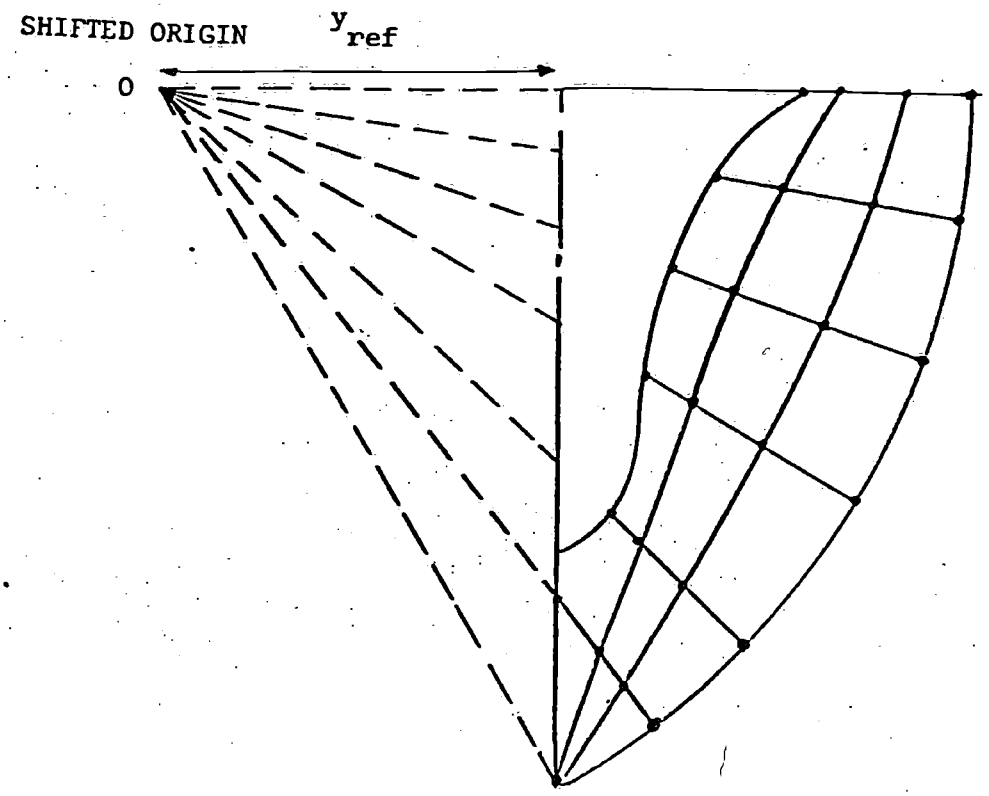

Fig. 3 The modified distorted cylindrical system with shifted origin

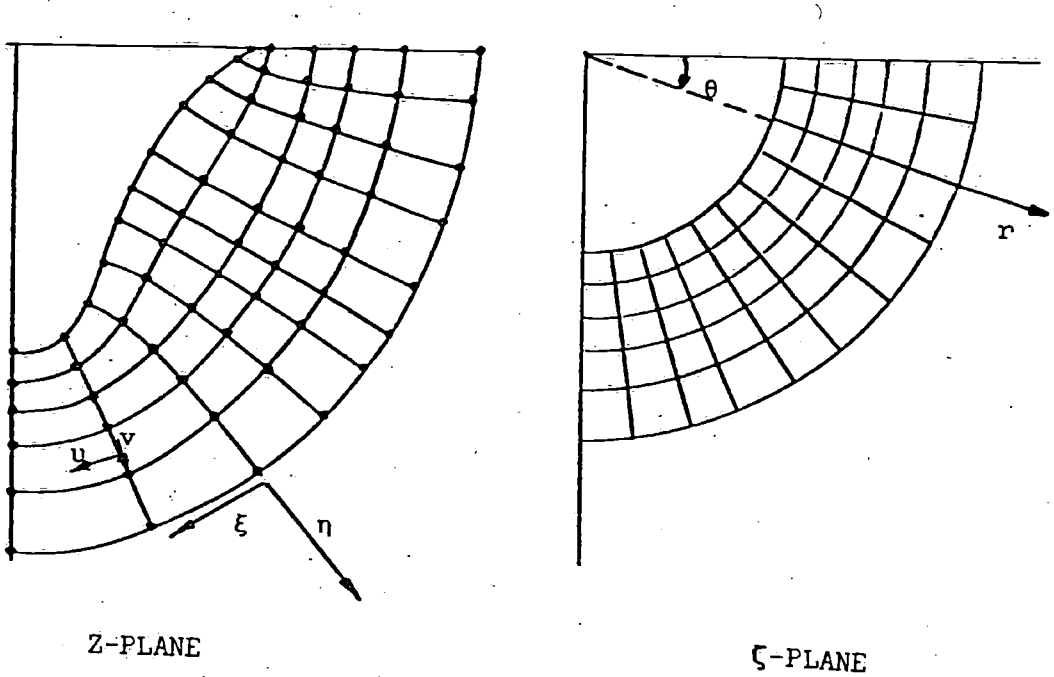

Fig. 4 The orthogonal curvilinear grid for a ship section

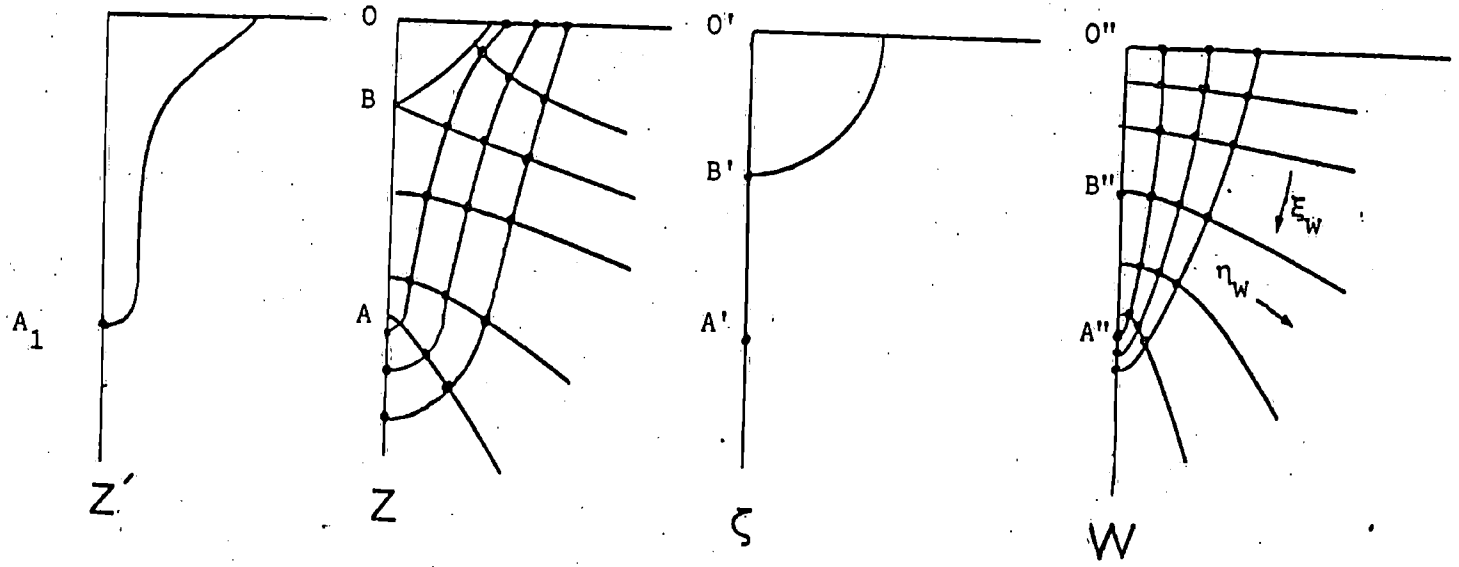

Fig. 5 The orthogonal curvilinear grid for stern and wake sections

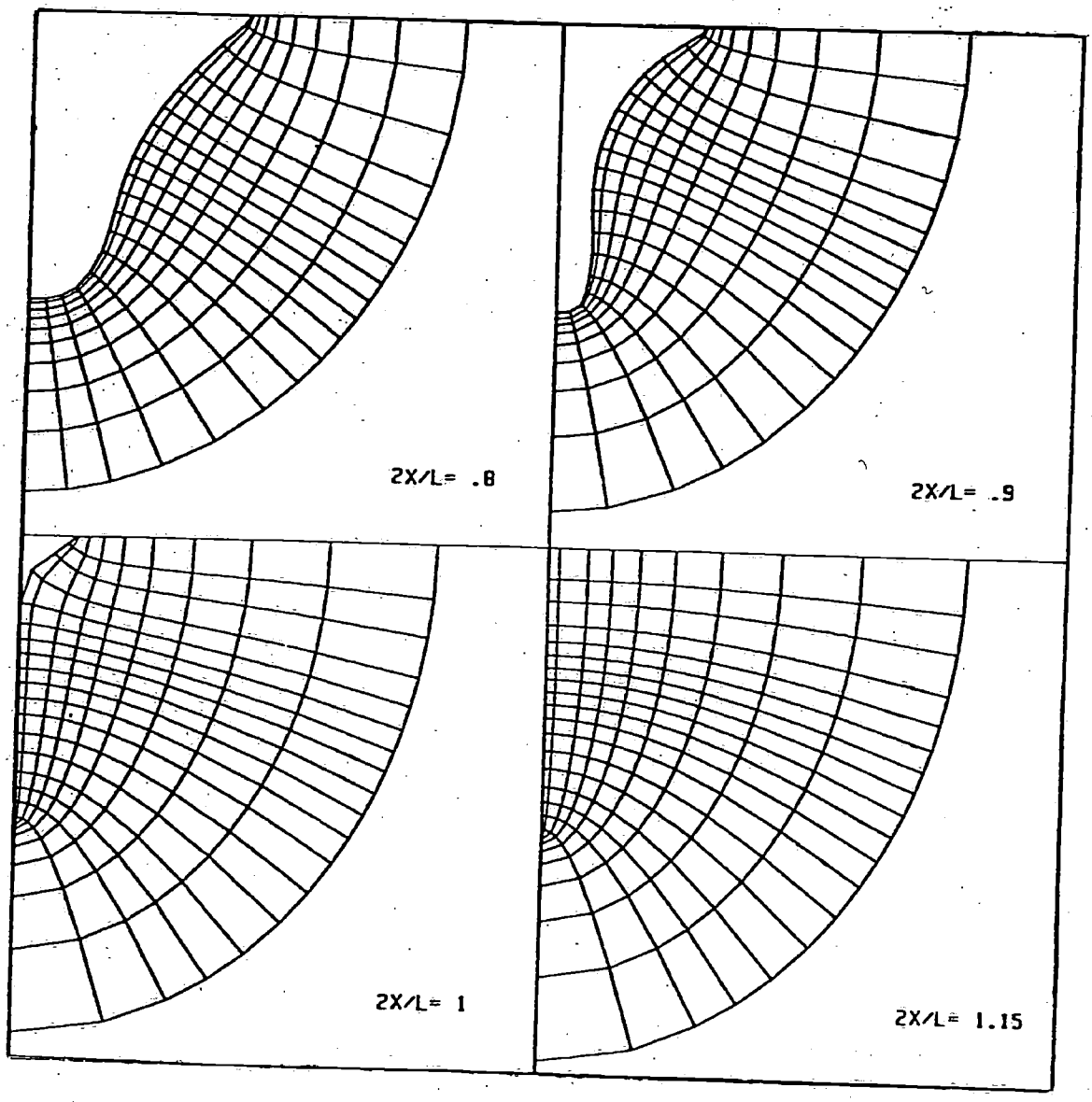

Fig. 6 Four orthogonal curvilinear grids for stern sections of the SSPA model

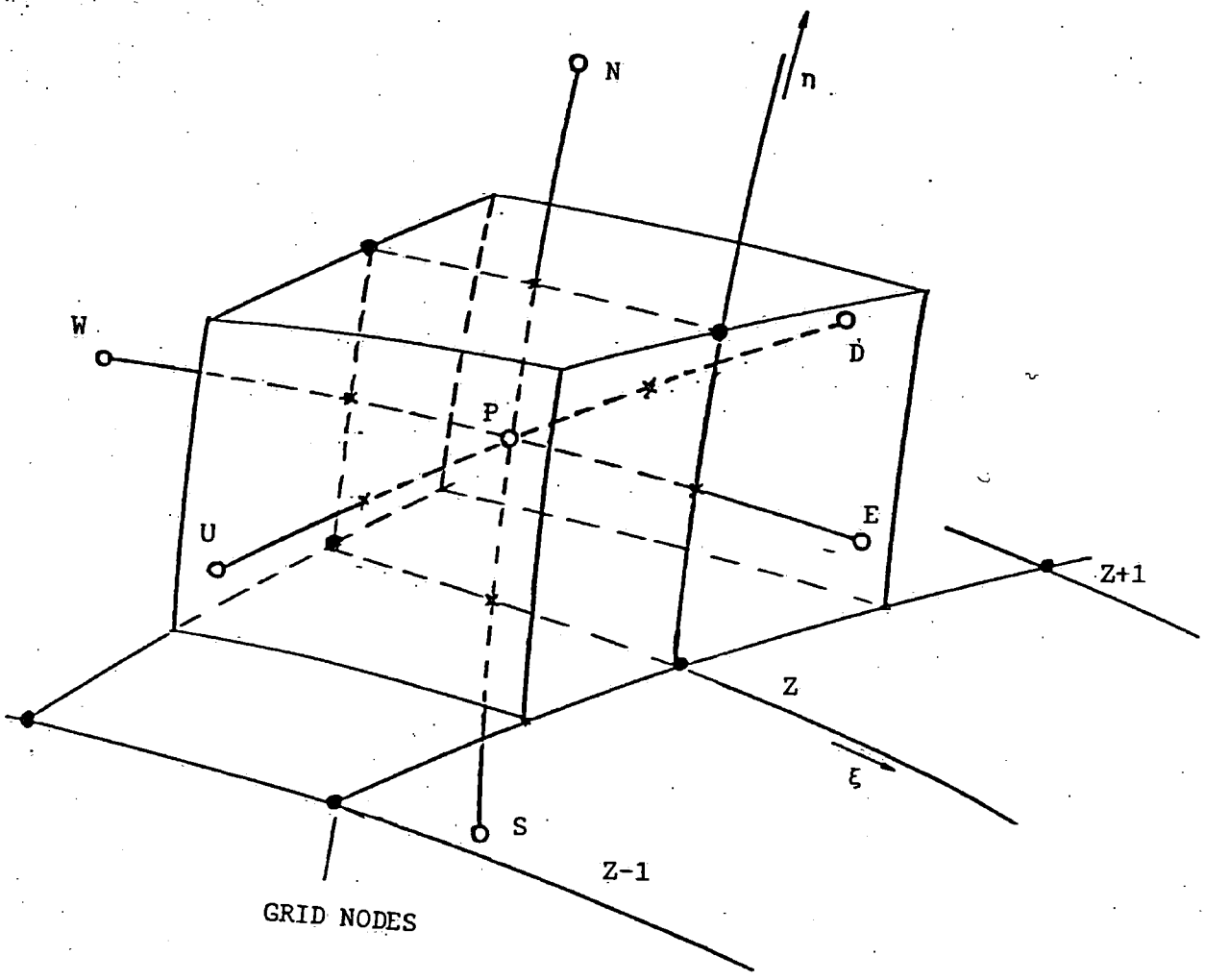

Fig. 7 The main control volume

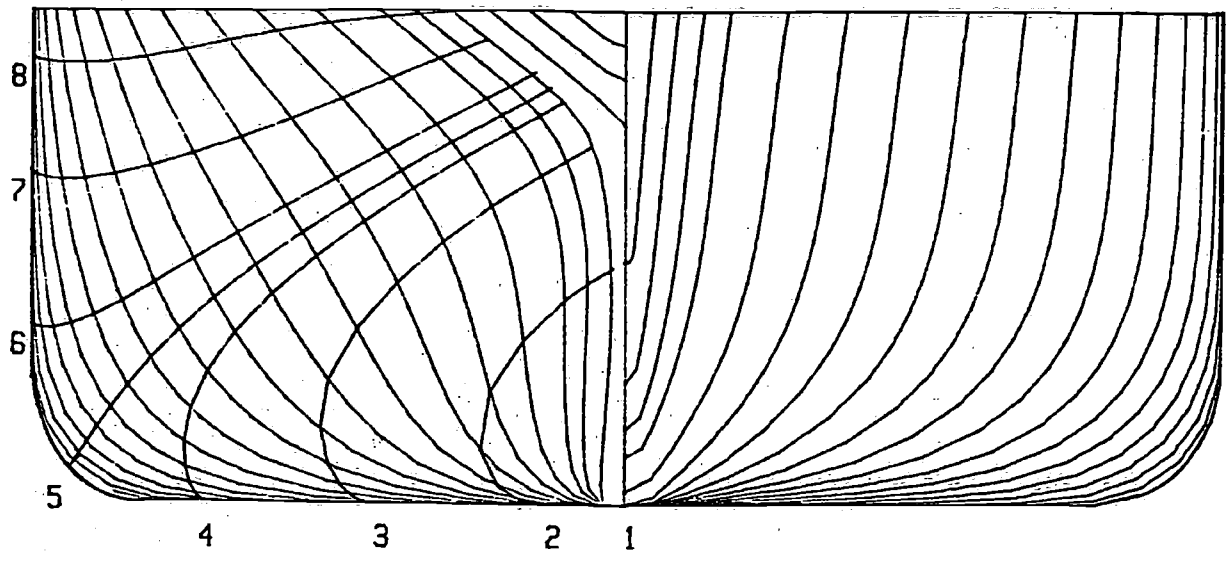

SSPA MODEL

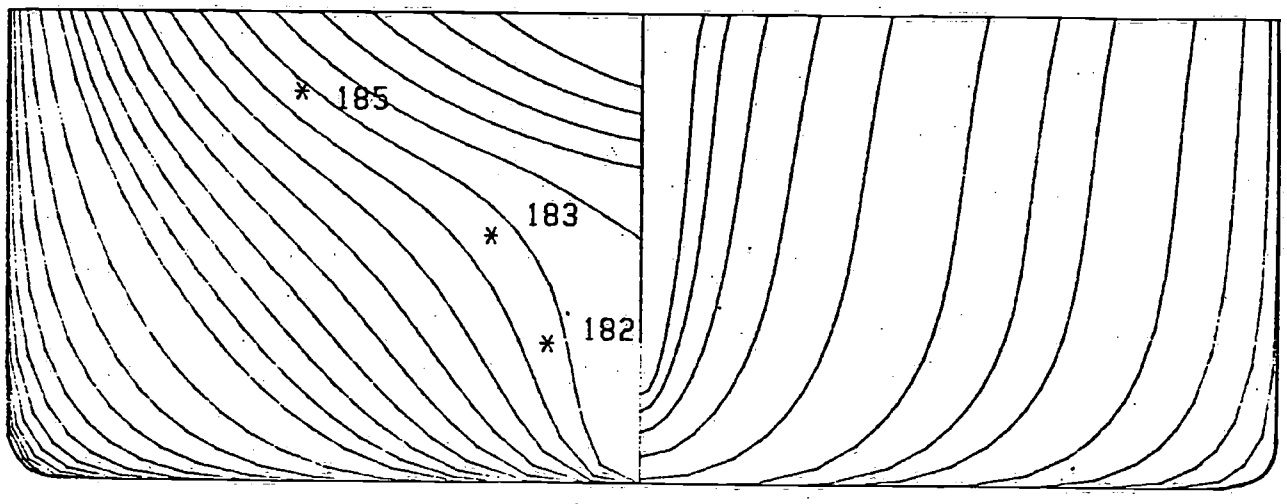

HSVA MODEL

Fig. 8 The Body Plans of SSPA and HSVA models

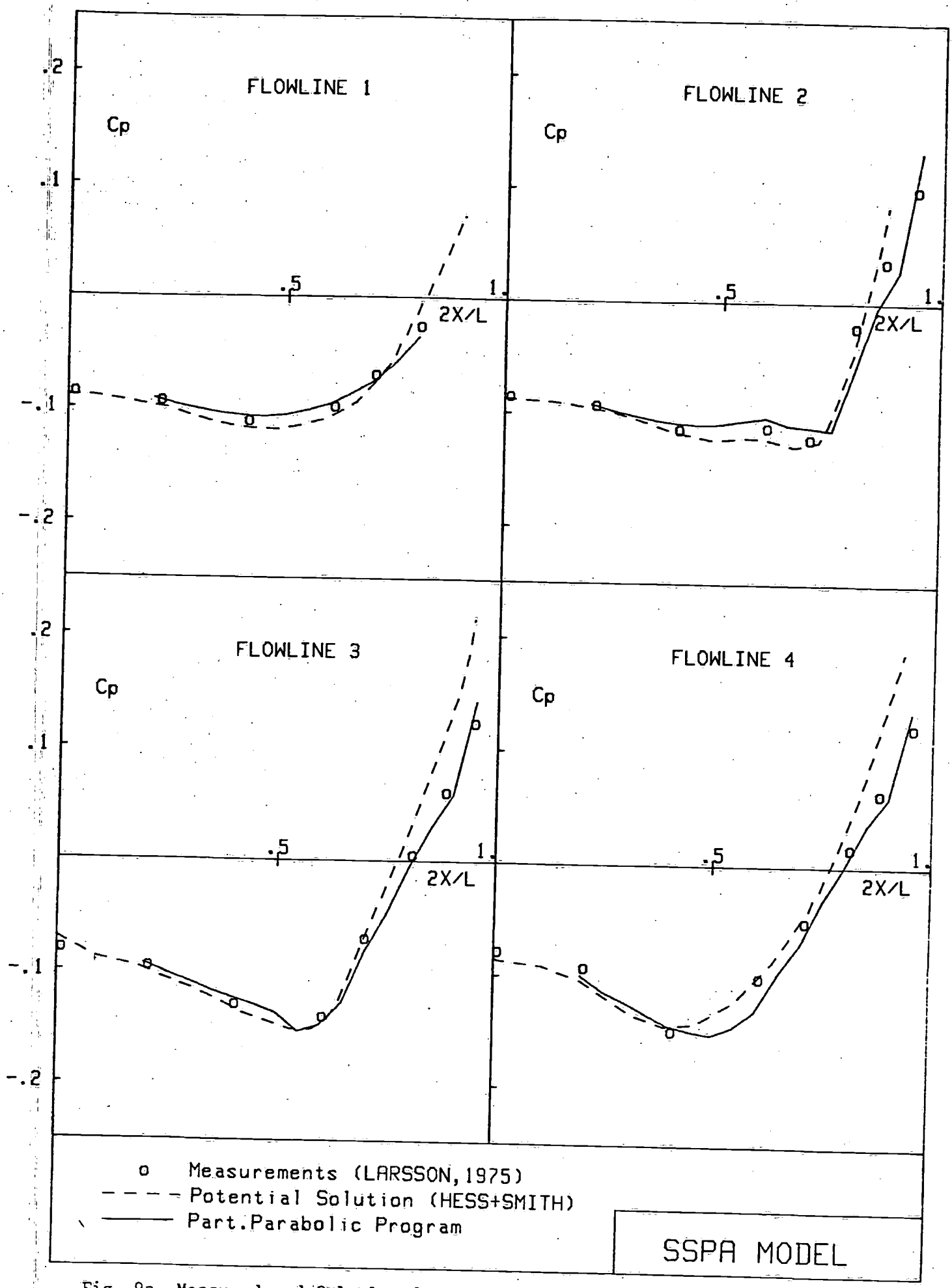

Fig. 9a Measured and Calculated values of C_p for the SSPA model

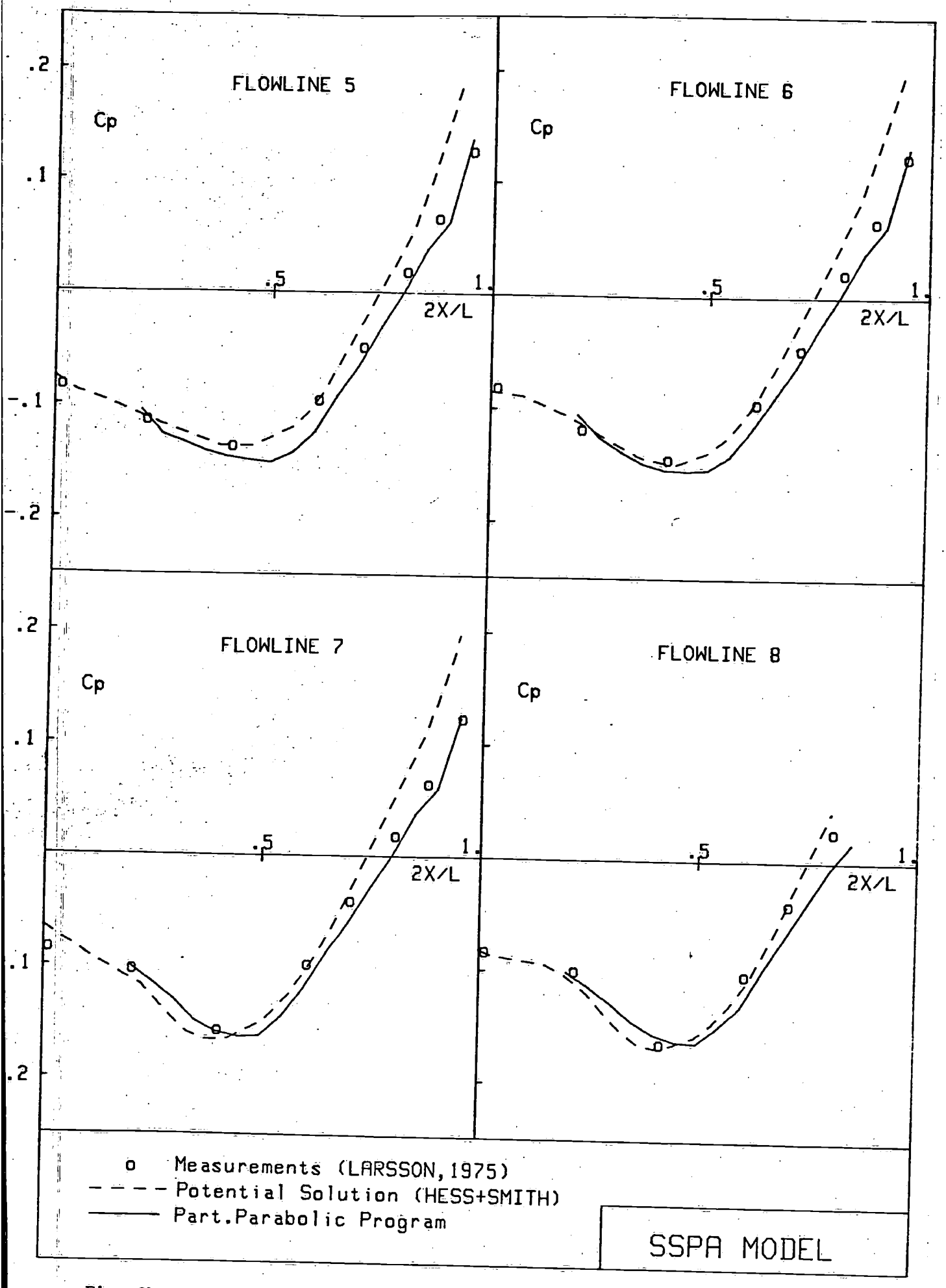

Fig. 9b Measured and Calculated values of C_p for the SSPA model

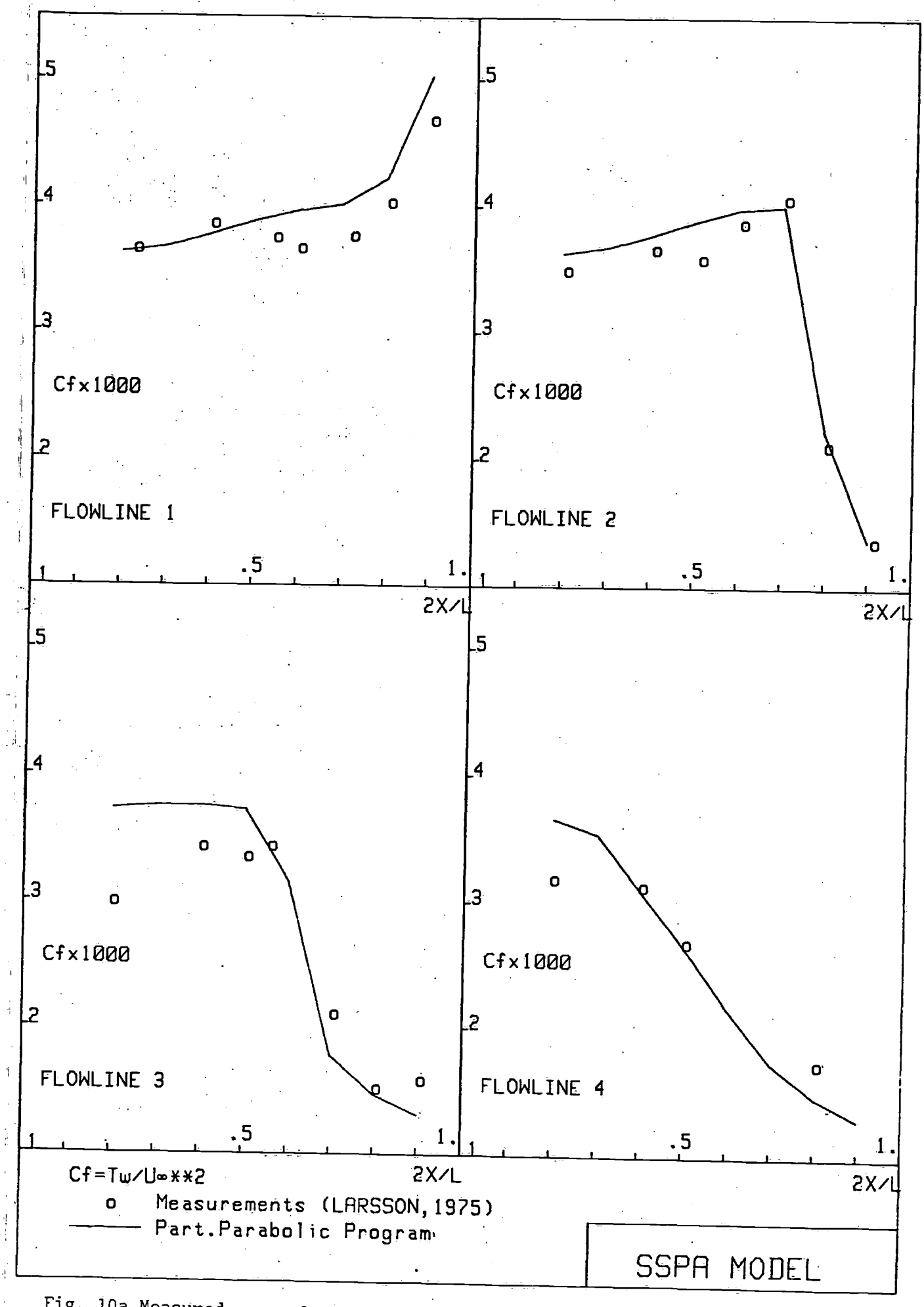

Fig. 10a Measured anc calculated values of C_f for the SSPA model

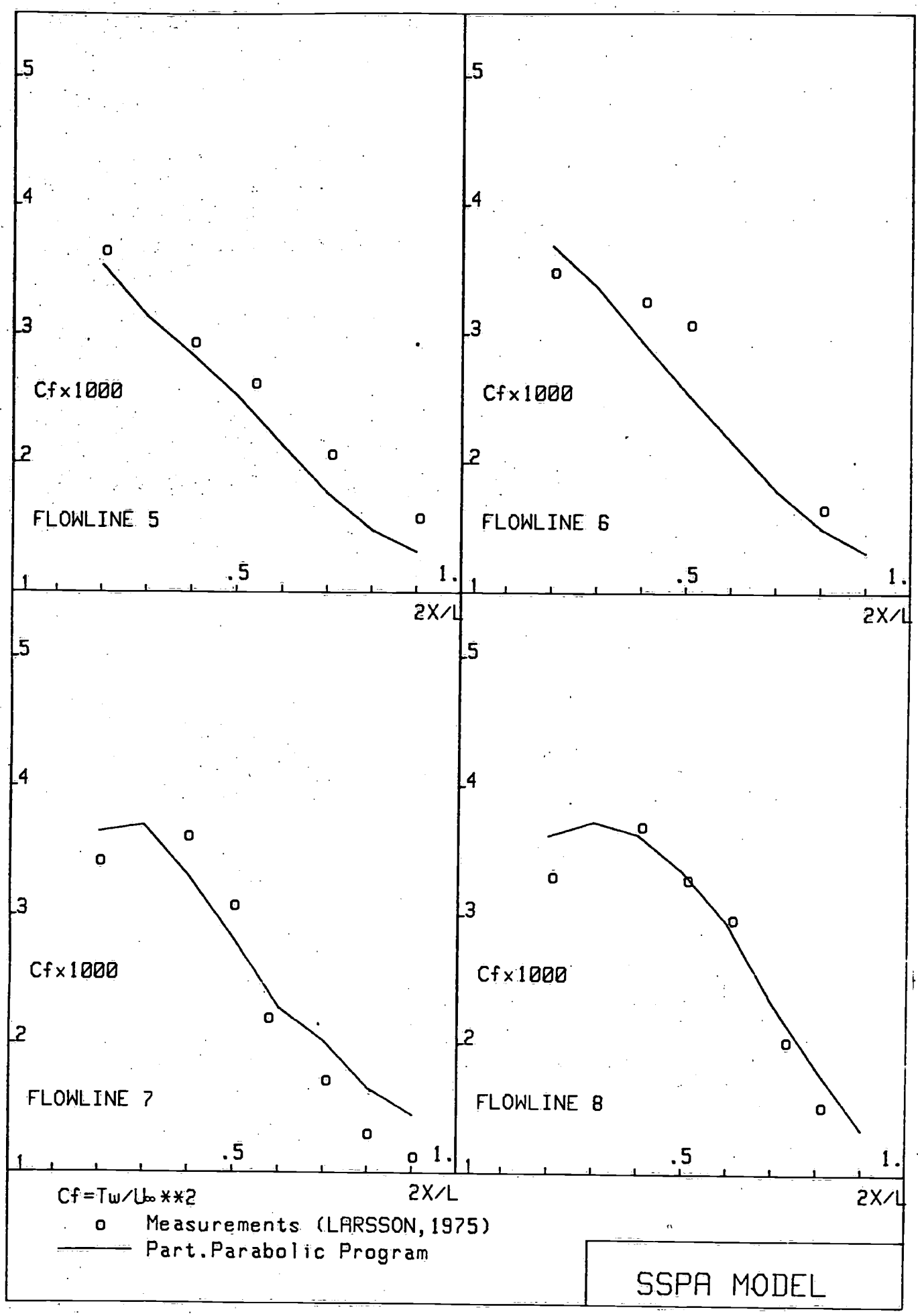

Fig. 10b Measured and calculated values of C_f for the SSPA model

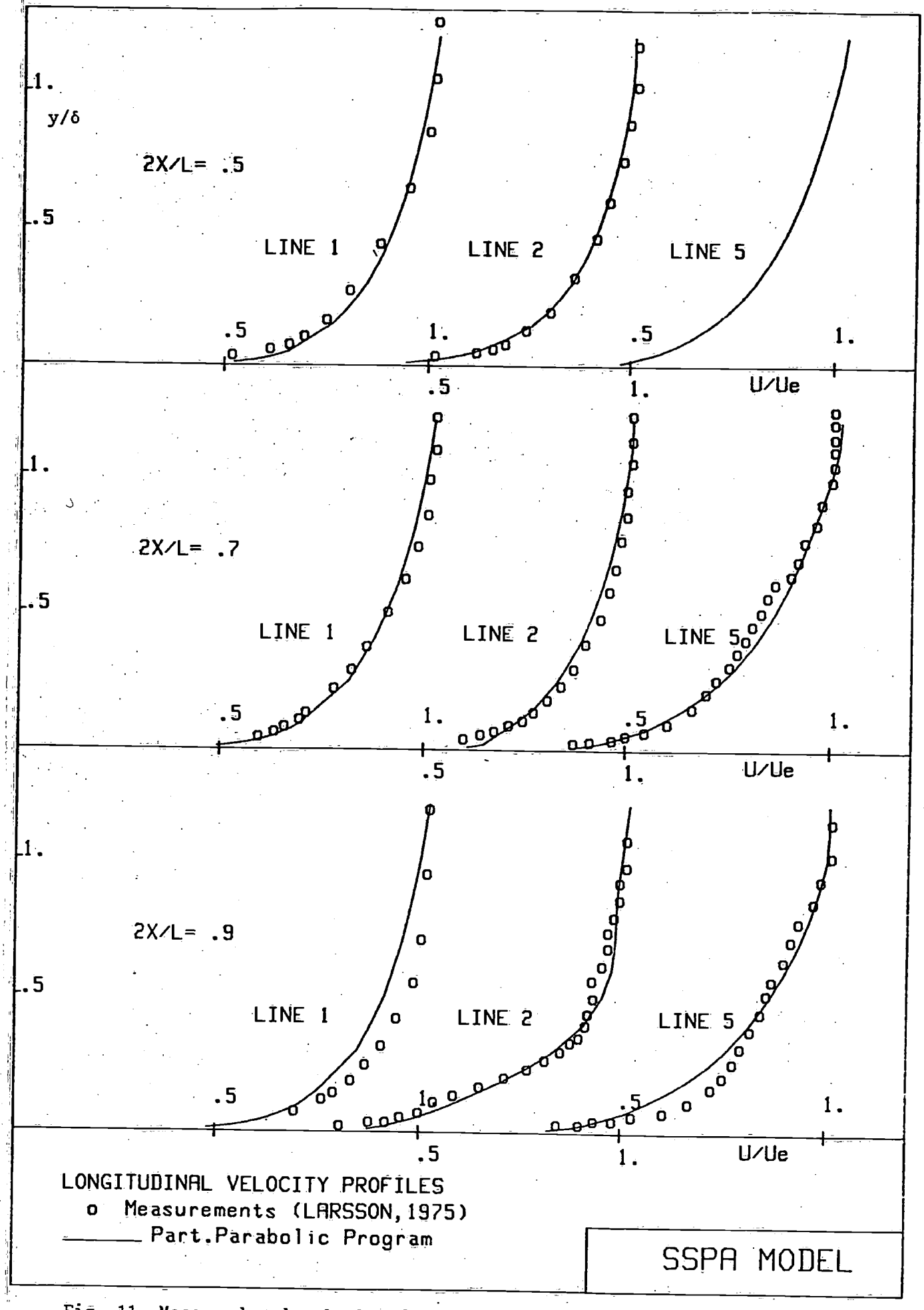

Fig. 11 Measured and calculated longitudinal velocity profiles for the SSPA model

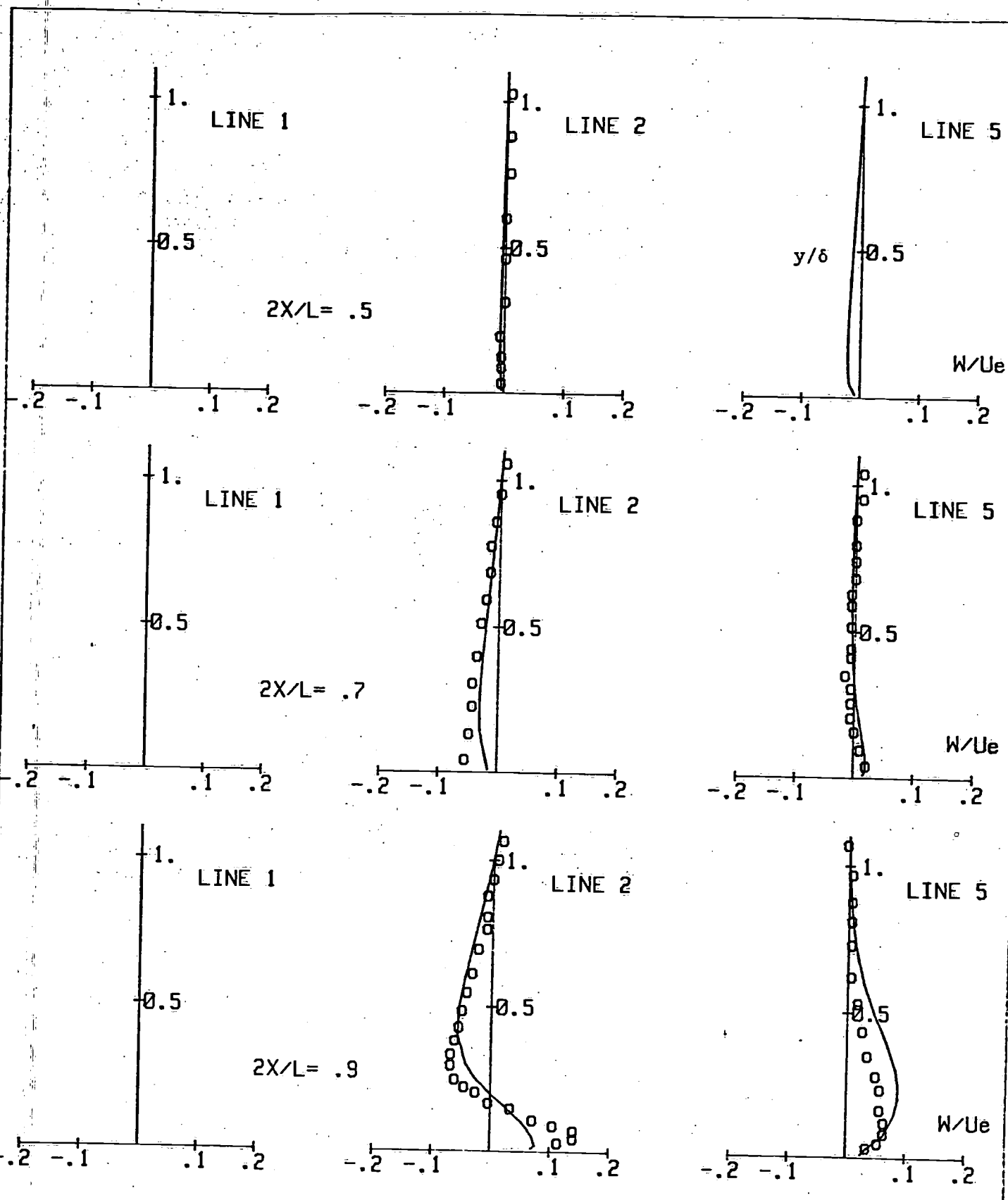

Fig. 12 Measured and calculated crosswise velocity profiles for the SSPA model

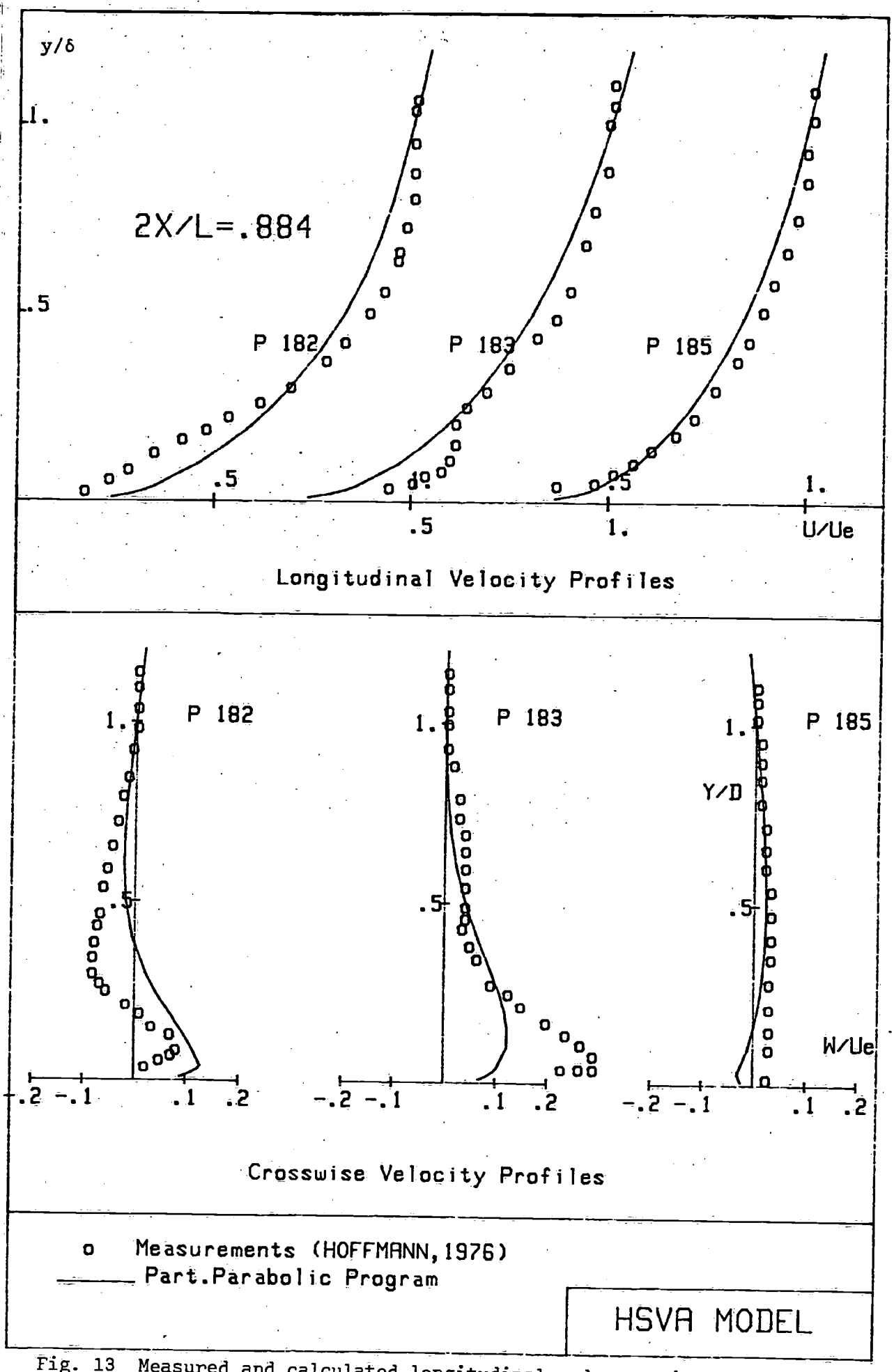

Fig. 13 Measured and calculated longitudinal and crosswise velocity profiles for the HSVA model

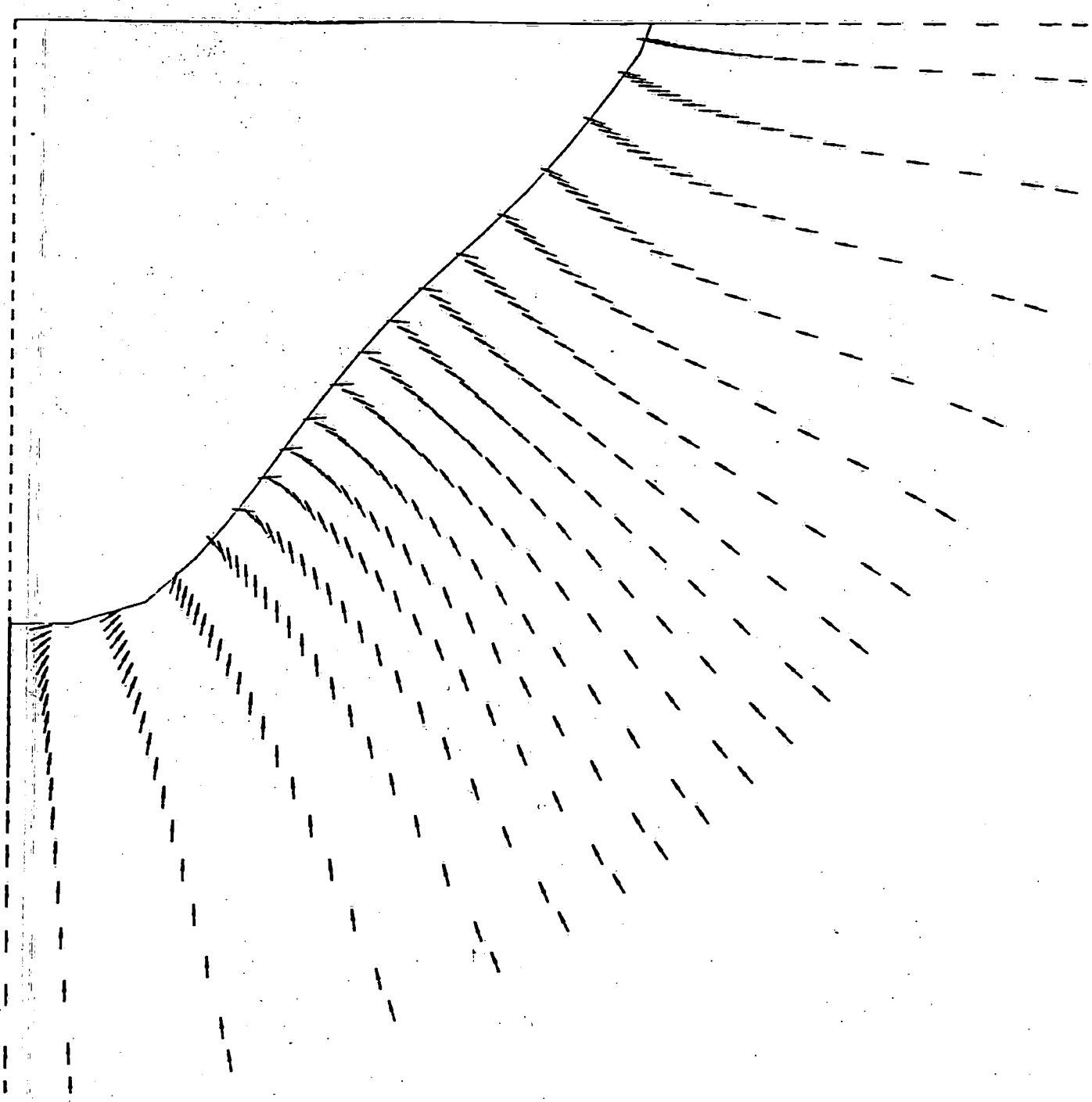

Fig. 14a Directions of crossflow velocities: HSVA model 2X/L =.825

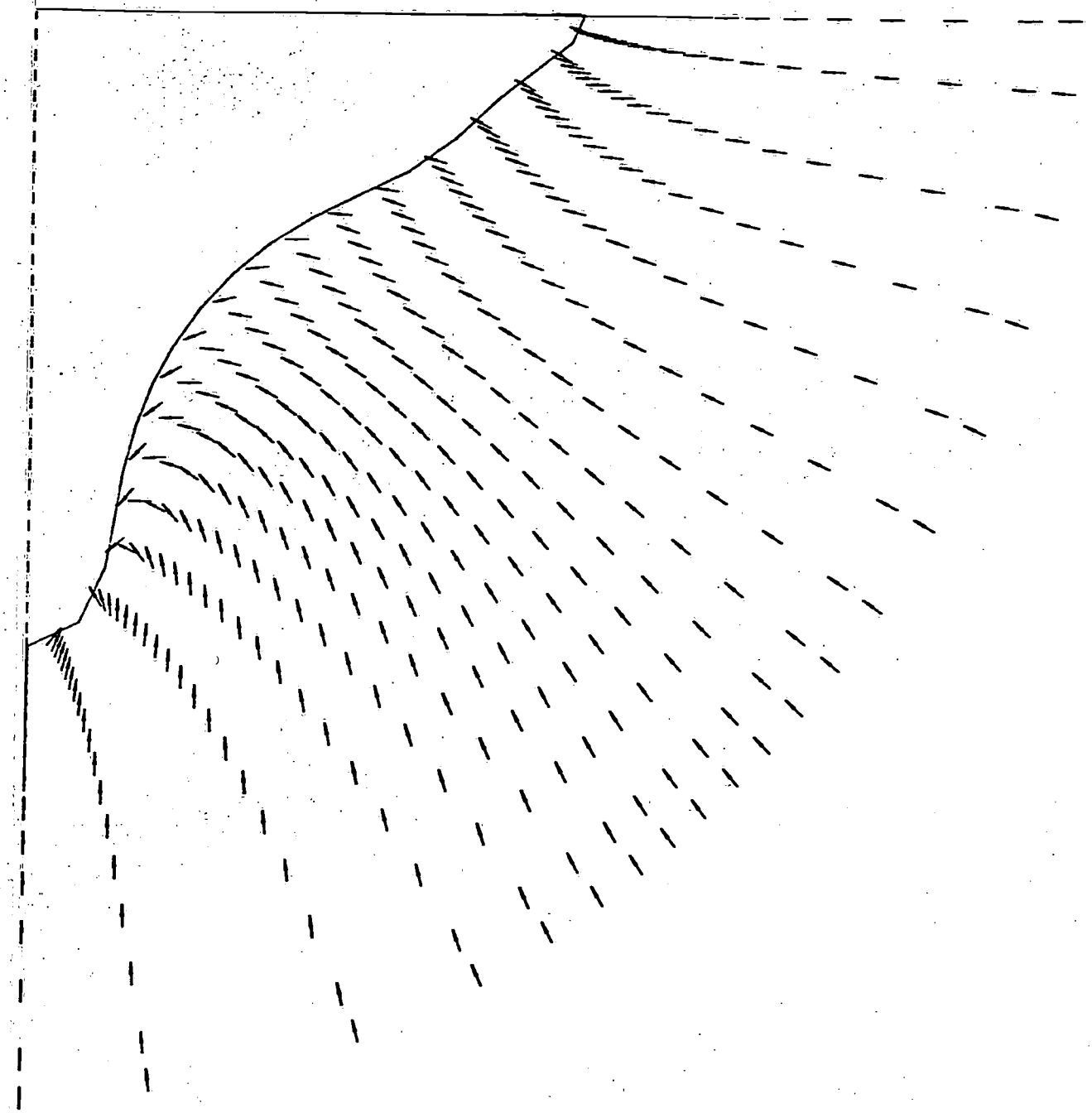

Fig. 14b Directions of crossflow velocities: HSVA model 2X/L =.9

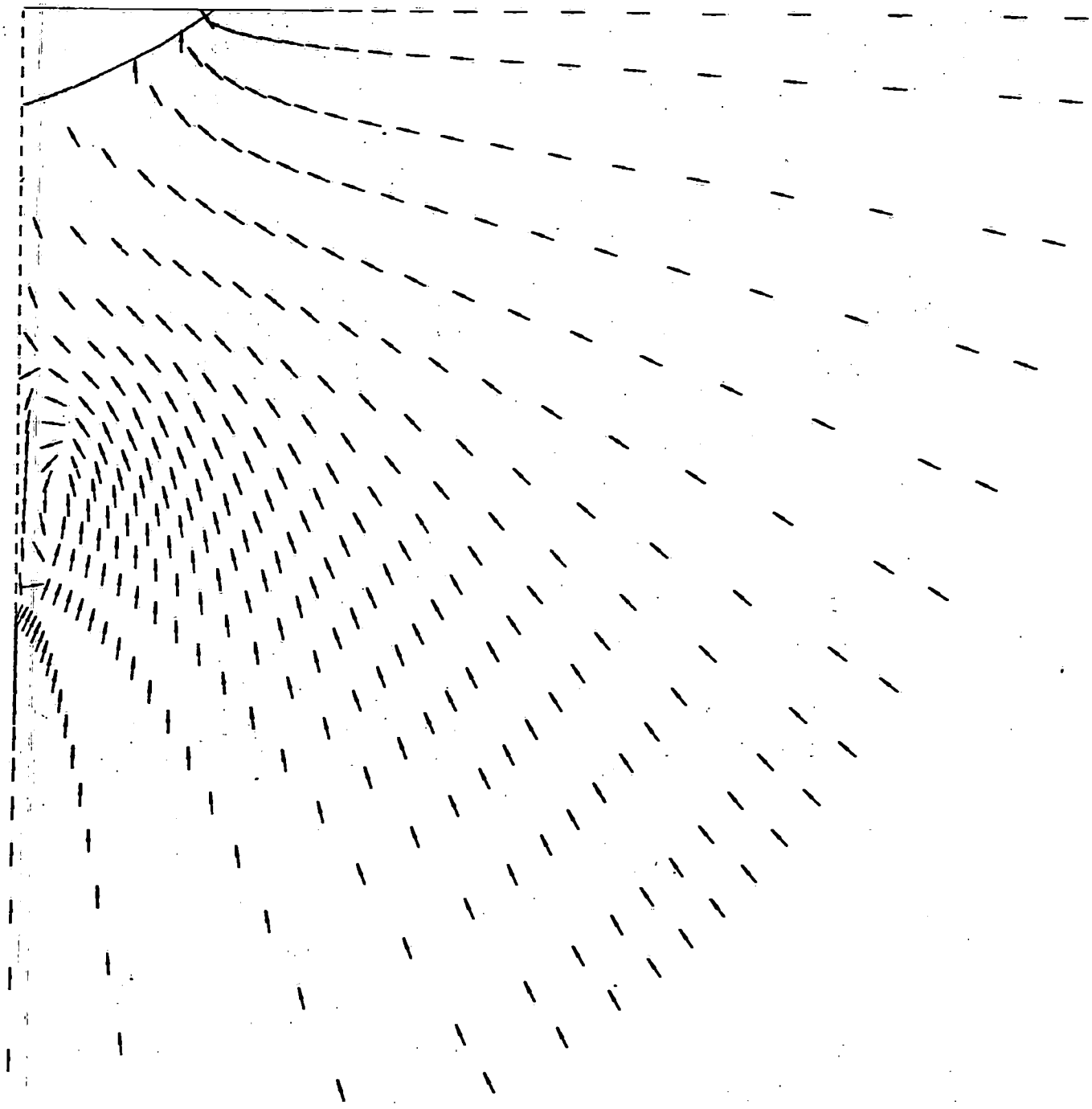

Fig. 14c Directions of crossflow velocities: HSVA model 2X/L = 1.025

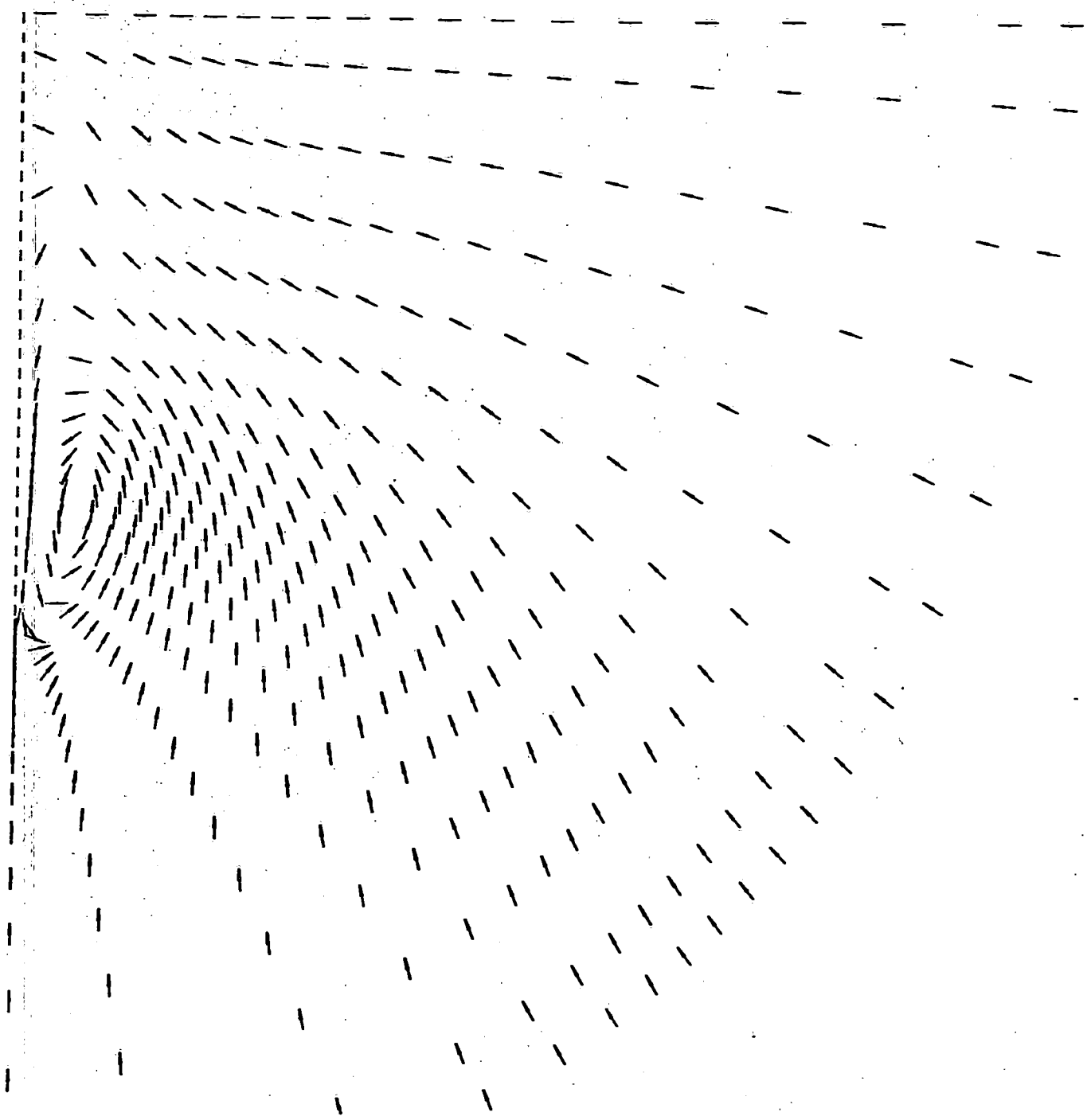

Fig. 14d Directions of crossflow velocities: HSVA model 2X/L = 1.075